

# ***Retraction***

## **Retraction Notice**

***Experimental Biology and Medicine* 2020; 0: 1. DOI: 10.1177/1535370219899031**

---

At the request of the authors, the following article has been retracted:

Yang X, Zhu X, Tang X, Liu M, Zheng H, Zheng L. Astragalus polysaccharides meliorate cardiovascular dysfunction in iron-overloaded thalassemic mice. *Exp Biol Med* (Maywood). 2019 Oct;244(14):1202-1209. doi: 10.1177/1535370219876540.

The authors notified the Editor-in-Chief that some of the data included in this paper is incorrect and therefore results may be unreliable. For this reason, the article has been retracted.

## RETRACTED: Astragalus polysaccharides meliorate cardiovascular dysfunction in iron-overloaded thalassemic mice

Xue Yang , Xiaoxi Zhu, Xianying Tang, Mei Liu, Huiling Zheng and Lin Zheng

Department of Eugenics and Genetics, Guiyang Maternal and Child Health-Care Hospital, Guiyang 550003, China  
Corresponding author: Xue Yang. Email: gsyangxue@163.com

### Impact statement

Currently iron chelation therapy is the standard treatment to inverse the iron-overload in thalassemia patients. However, inevitable side effects along with passable cardio-protective efficacy have been reported. In this study, astragalus polysaccharides (APS) treatment effectively attenuated cardiovascular dysfunction via regulating oxidative stress in  $\beta$ -thalassemic mice, while the levels of cardiac apoptotic proteins remained unchanged. Our study highlights the therapeutic potentials of APS in the treatment of iron-overloaded disorders.

### Abstract

Astragalus polysaccharides (APS) are well-known oriental herbal medicine ingredients with various bioactivities. Herein we aimed to explore the regulation of APS in the iron overloaded  $\beta$ -thalassemic mice. Iron diet was provided to induce iron-overload condition in wild-type and  $\beta$ -thalassemic mice, to which APS was administered by gavage. The heart weight index, hemoglobin, left ventricular function, heart rate variability (HRV), cardiac iron and malondialdehyde, reactive oxygen species (ROS) and cardiac apoptotic proteins including Bax, Bcl-2, and caspase3 were detected among different mouse groups. Iron overload led to the impaired left ventricular function and HRV, plasma non-transferrin-bound iron, ROS, and cardiac mitochondrial function in thalassemic mice. Our data suggested that in thalassemic mice with iron-overload, APS administration showed benefits in alleviating iron accumulation and oxidative stress, ameliorating HRV and left ventricular function, without altering the cardiac apoptosis proteins. Our results demonstrated that APS effectively attenuated cardiovascular dysfunction via regulating oxidative stress, while the levels of cardiac apoptotic proteins remained unchanged.

**Keywords:**  $\beta$ -thalassemic, heart rate variability, oxidative stress

*Experimental Biology and Medicine* 2019; 244: 1202–1209. DOI: 10.1177/1535370219876540

### Introduction

Beta-thalassemia is an inherited blood disease characterized by the absent or reduced beta globin subunit of hemoglobin, often resulting in chronic hemolytic anemia.<sup>1,2</sup> Beta-thalassemia is prevalent in multiple regions including Southeast Asia, Mediterranean, Middle East and North India.<sup>3</sup> Anemic patients typically rely on regular blood transfusion, which often causes iron-overload-related cardiomyopathy, accounting for the morbidity and mortality of cardiac dysfunction in beta-thalassemia patients.<sup>3</sup> In addition, excess iron can cause serious and irreversible organ damages and disorders such as cirrhosis, diabetes, and hypogonadism.<sup>4</sup>

Currently, iron chelation therapy is the standard treatment to inverse the iron-overload in thalassemic patients, along with the inevitable side effects and passable cardio-protective efficacy.<sup>5</sup> There is a strong need for the development of alternative therapeutic strategy for

iron-overload. To patients suffering from iron-overload cardiac complications, the major reason is the excess iron accumulation in the heart,<sup>6</sup> which results in increased reactive oxygen species (ROS) production in the cardiac mitochondria dysfunction. Previous study also showed that ROS could be responsible for cardiac failure induced by the chronic iron overload.<sup>7,8</sup>

Astragalus polysaccharides (APS) is one of the main functional ingredients extracted from the root of Chinese herbal *Astragalus membranaceus*, which has been widely used in the treatment of heart failure.<sup>9</sup> APS exerts various bioactivities including pro-angiogenic, anti-inflammatory properties, relating to their protective effects in different disease models. For instance, APS administration was able to alleviate heart dysfunction symptoms in streptozotocin-induced diabetic mice by reducing oxidative stress/damage.<sup>10</sup> APS could also relieve the increase of the cell volume in myocardium, and reduce cell apoptosis in

rodent models.<sup>3</sup> These models have provided extensive information on mechanisms, and prompted specific hypotheses about the effect of cancer treatment on any regions of the gastrointestinal tract.<sup>3</sup> However, there are challenges associated with rodent models including being prohibitively expensive, time consuming, and the relative difficulty of genetic manipulation. *In vitro* models are also utilized to study gastrointestinal toxicity. Epithelial cell lines derived from the intestine are cultured as monolayers, in an attempt to mimic the intestinal epithelium.<sup>4</sup> However, there are many limitations to *in vitro* work, and while they can be useful to understand simple mechanisms, they lack stromal, neural, and immune signaling which is of key importance for modeling gastrointestinal toxicity. Further, they cannot recapitulate the complex systemic metabolism of compounds and thus do not assay the full spectrum of compound derivatives found *in vivo*. Considering the constraints of *in vivo* and *in vitro* models currently used, an alternative model to study cancer treatment-induced gastrointestinal toxicity that allows rapid, miniaturized, multi-organ toxicity, screening-amenable testing is warranted.

Recently, a new zebrafish transgenic eGFP reporter, *Tg(cyp2k18:egfp)*, was developed by identifying highly upregulated genes as biomarkers of liver toxicity.<sup>5</sup> Although this transgenic zebrafish reporter line was initially developed for liver toxicity, upon further testing, it was identified that the line also induced eGFP in the gastrointestinal tract following drug treatment, highlighting this organ as a major detoxification site. Detailed investigations have also reported the intestinal morphology and genetic expression of the zebrafish, demonstrating it as a useful model for gastrointestinal disease models.<sup>6–8</sup> Transcriptome profiling has demonstrated that the large anterior portion (58%) of the zebrafish intestine has a similar RNA profile to the human small intestine, followed by a small transitional zone (14%), a tissue resembling the caecum (14%) and lastly a profile resembling the rectum (14%).<sup>8</sup> Zebrafish do not have separated stomach or colon sections, and instead have a continuous tube with segments expressing some genes characteristic of human colon and rectum.<sup>8</sup>

Here we exploit this newly developed transgenic zebrafish reporter line to investigate its utility as an alternative vertebrate model to bridge the gap between simple *in vitro* cellular studies and complex *in vivo* models for understanding gastrointestinal toxicity induced by SN38 and afatinib. These agents are associated with high levels of gastrointestinal toxicity, manifesting as diarrhea, and represent two classes of anti-cancer agents; classical cytotoxic chemotherapy (SN38, a topoisomerase 1 inhibitor) and targeted agents (afatinib, a pan-HER tyrosine kinase inhibitor).<sup>9–13</sup> Thus, this study aimed to assess the efficacy of zebrafish as a platform to study gastrointestinal toxicity second to anti-cancer chemotherapy and targeted therapy.

## Materials and methods

### Fish husbandry

Experiments were conducted under the authority of the Institutional Animal Care and Use Committee (IAUCUC)

of the Biological Resource Centre, A\*STAR (Protocol number 120751), mandated by National Advisory Committee for Laboratory Animal Research Guidelines of the Agri-Food and Veterinary Authority, Singapore.

Zebrafish (*Danio rerio*) were housed in the zebrafish facility of the Institute of Molecular and Cell Biology, a division of A\*STAR, Singapore. Larvae were obtained through natural crosses and staged as previously described by Kimmel *et al.*<sup>14</sup> Embryos and larvae were raised and treated in water containing 60 µg/mL sea salt (Red Sea Aquatics, UK), and 1% methylene blue.

Zebrafish used included wildtype (AB strain), *Tg(cyp2k18:egfp)* reporter line and *Tg(BACmpx:gfp)* reporter line. The development of both the *Tg(cyp2k18:egfp)* reporter line and *Tg(BACmpx:gfp)* line have been described previously.<sup>5,15</sup>

### Drug treatment

For treatment of both larvae and adults, SN38 (Tocris bio-science, 2684) was used as the chemotherapeutic agent, and afatinib (AdooQ, A10141) was used as the HER-TKI agent. Both were administered to mimic clinical administration (afatinib orally, and SN38 via intraperitoneal injection). Diclofenac (Sigma D6899) was used as the positive control to cause hepatic and gastrointestinal toxicity reported by *Tg(cyp2k18:egfp)* zebrafish line (larvae only). Larvae were treated at three days post fertilization (dpf). Drug compounds were dissolved in DMSO, and added to the egg water in a 12-well plate (volume 2 mL/well), with 10 larvae/well. All treatments were conducted in duplicate. Compounds were dissolved in DMSO, and diluted in egg water for larvae treatment. DMSO exposure to larvae or adult fish did not exceed 0.01%. SN38 and afatinib were administered to larvae at a range of concentrations from 0.5 to 900 µM for 24 hours, and optimal dose for treatment was determined as 300 µM. Positive controls (*Tg:cyp2k18* line only) were administered diclofenac at a concentration of 13 µM for 24 h as this is known to induce eGFP in this line.<sup>5</sup> Controls were administered the corresponding solvent concentration (DMSO, 0.01%).

Adult zebrafish were weighed and administered 10, 20, 30, and 40 µg/g afatinib via oral gavage, with the maximum volume administered not exceeding 1% of the fish body-weight. Afatinib was dissolved in DMSO, and diluted in PBS. DMSO exposure did not exceed 0.01%. Controls were administered the corresponding solvent concentrations (DMSO, 0.01%). The oral gavage technique was modified from Collymore *et al.*<sup>16</sup> A soft, flexible 20 µL ultra-micro tip (eppendorf) was trimmed to 5 cm in total length, and the cut edge was assessed under a dissection microscope to ensure cut edges were blunt, with no beveled or sharp edges. A sponge was cut with a groove and soaked in facility system water to hold zebrafish during gavage procedure. The ultra-micro tip was attached to a pipette and appropriate volume drawn up, ensuring no bubbles were present, and gently inserted into mouth, below the gills. To ensure procedure was effective, Casper transparent zebrafish<sup>17</sup> were gavaged with phenol red (1:10 dilution with a 0.5% phenol red solution in Dulbecco's PBS). This indicated

that the solution was entering the intestinal bulb and not exiting via the gills, and that fish did not expel the solution through their mouth (Supplementary Figure 1). Fish were killed 24 h following gavage.

Adult zebrafish were weighed and administered 10, 20, 30, 40  $\mu\text{g/g}$  SN38 via intraperitoneal injection, with the maximum volume administered not exceeding 1% of the fish bodyweight. SN38 was dissolved in DMSO, and diluted in PBS. DMSO exposure did not exceed 0.01%. Controls were administered the corresponding solvent concentrations (DMSO, 0.01%). Using a 10  $\mu\text{L}$  micro syringe (Hamilton), the correct volume was injected into the fish on the ventral body wall, posterior to the pelvic girdle and anterior to the anus, roughly midway along the length of a pelvic fin. The tip of the needle was pointing rostrally, and was inserted shallowly. Fish were killed 24 h following injection.

### Imaging and tissue preparation

For imaging, larvae were anaesthetized with 0.02% Tricane (buffered to pH 7.0) and placed on a Petri dish under a Leica MZ16FA. Only larvae were imaged for eGFP induction as they are transparent.

Adult fish were culled by placing in 0.02% Tricane. A shallow longitudinal incision on the ventral side, from the gills to the anus, was made to remove the intestines which were uncoiled and the anterior 60% of the intestines were fixed in 4% PFA overnight before processing and embedding in paraffin.

### Histopathological analysis

Hematoxylin and eosin (H&E) staining was performed on 4  $\mu\text{m}$  sections of intestine, cut on a rotary microtome and mounted onto glass Superfrost<sup>®</sup> microscope slides (Menzel-Gläser, Braunschweig, Germany). Slides were scanned using a NanoZoomer<sup>™</sup> (Hamamatsu Photonics, Japan) and assessed with NanoZoomer Digital Pathology software view.2 (Histalim, Montpellier, France). The occurrences of six histological criteria in the intestine were examined to generate a total tissue injury score.<sup>18</sup> These criteria were villous fusion, villous atrophy, disruption of brush border and surface enterocytes, infiltration of polymorphonuclear cells and lymphocytes, dilation of lymphatics and capillaries, and edema. Each parameter was scored as present = 1, or absent = 0, in a blinded fashion (YZAVS).

### Goblet cell analysis

Alcian blue (1% Alcian blue 8GX (CI 74240) in 3% glacial acetic)/periodic acid Schiff staining was performed on 4  $\mu\text{m}$  sections the intestine. Sections were oxidized in 1% periodic acid before washing then treated in Schiff's reagent. Slides were scanned using a NanoZoomer<sup>™</sup> (Hamamatsu Photonics, Japan) and assessed with NanoZoomer Digital Pathology software view.2 (Histalim, Montpellier, France). Data presented as average per villus. All analysis was done in a blinded fashion (YZAVS).

### Immunohistochemistry

Immunohistochemical analysis was performed for apoptosis analysis (caspase 3; BD Pharmingen #559565). Change in caspase-3 is a validated marker for altered tissue kinetics in previous models of cancer therapy-induced gastrointestinal toxicities.<sup>19–22</sup> Immunohistochemical analysis was performed using Dako reagents on an automated machine (AutostainerPlus<sup>™</sup>, Dako, Denmark) following standard protocols supplied by the manufacturer. Briefly, sections were deparaffinized in histolene and rehydrated through graded ethanol before undergoing heat-mediated antigen retrieval using an EDTA/Tris buffer (0.37 g/L EDTA, 1.21 g/L Tris; pH 9.0). Retrieval buffer was preheated to 65°C using the Dako PT LINK (pre-treatment module). Slides were immersed in the buffer and the temperature raised to 97°C for 20 min. After returning to 65°C, slides were removed and placed in the Dako AutostainerPlus and stained following manufactures guidelines. Negative controls had the primary antibody omitted. Caspase 3 was quantified by counting the number of positively stained cells. Data presented as average positively stained cells per villus. All analysis was done in a blinded fashion (YZAVS).

### Statistics

Data were compared using Prism version 7.0 (GraphPad<sup>®</sup> Software, San Diego USA). A D'Agostino Pearson omnibus test was used to assess normality. When normality was confirmed, a one-way analysis of variance (ANOVA) with appropriate post hoc testing was performed to identify statistical significance between groups. In other cases, a Kruskal-Wallis test with Dunn's multiple comparisons test and Bonferroni correction was performed. Differences were considered significant when  $P < 0.05$ .

## Results

### Dose titration

**Larvae zebrafish.** Zebrafish larvae ( $n = 10/\text{group}$ ) were treated with varying doses of afatinib and SN38, ranging from 100  $\mu\text{M}$  to 1 mM to determine optimal treatment dose. SN-38 did not cause mortality in larvae at any concentration tested. In contrast, afatinib induced dose-dependent mortality (Figure 1). The optimal dose of afatinib for larvae was determined as LC25 (300  $\mu\text{M}$ ).

**Adult zebrafish.** Adult zebrafish ( $n = 6/\text{group}$ ) were treated with SN38 (by intra peritoneal injection) or afatinib (by oral gavage) at 10, 20, 30, and 40  $\mu\text{g/g}$  based on previous publications.<sup>23</sup> SN-38 and afatinib did not cause mortality or noticeable morbidity in adult fish, and hence 40  $\mu\text{g/g}$  was dosed for the remainder of the study.

### Transgenic zebrafish larvae fluorescence imaging

To assess the effectiveness of zebrafish Tg(*cyp2k18:egfp*) reporter line as a high-throughput screening for gastrointestinal toxicity of cancer treatment, larvae were treated with SN38 and afatinib, anti-cancer compounds with

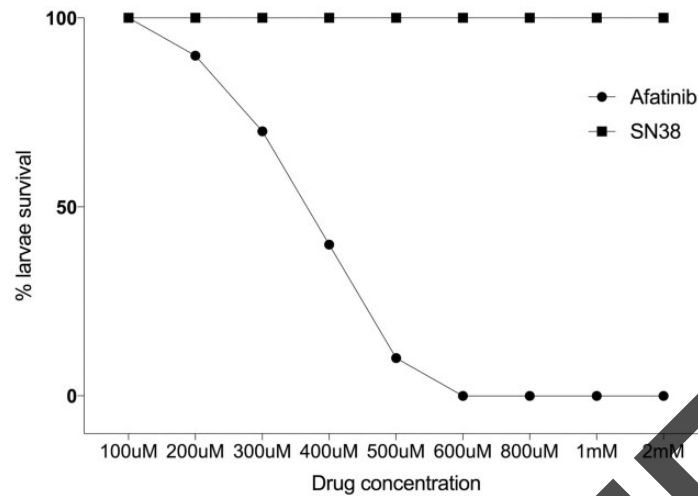


**Figure 1.** Percent death of larvae. Administration of varying concentrations of afinatib caused lethality in zebrafish larvae. At doses below 100  $\mu\text{M}$ , no larvae died. Doses above 600  $\mu\text{M}$  caused lethality in 100% of larvae. LC25 (dotted line) was 300  $\mu\text{M}$ , and this was determined as the optimal dose for further treatment. SN38 did not cause death at any concentration.

known gastrointestinal toxicity profiles; and positive control, diclofenac.<sup>5</sup> Larvae were imaged for induction of eGFP in the gastrointestinal tract of Tg(*cyp2k18:egfp*) reporter line. As expected, diclofenac induced eGFP in the gastrointestinal tract of the Tg(*cyp2k18:egfp*) zebrafish larvae (Figure 2(a)), whereas untreated, SN38 and afinatib did not elicit a response (Figure 2(b) to (d)). To assess gut inflammation, the neutrophil reporter line, Tg(*BACmpx:gfp*) was also exposed to both compounds. Untreated controls had neutrophils primarily contained in the vasculature, with  $11.6 \pm 0.88$  (mean  $\pm$  SEM) neutrophil cells outside of the vasculature (indicated by white arrow in untreated control, Figure 2(e)). A one-way ANOVA indicated that this was significantly less than treated larvae ( $P < 0.01$ ). SN38 and afinatib induced neutrophil translocation from the vasculature to surrounding tissues; however, this was not specific to the gastrointestinal tract (Figure 2(f) and (g)). Larvae treated with SN38 showed relatively fewer translocated neutrophils ( $49.6 \pm 3.92$ ) compared to afinatib-treated larvae ( $82.6 \pm 10.71$ ) ( $P = 0.013$ ).

### Histopathological intestinal analysis in adult zebrafish

To assess the effect of cancer drugs on the histopathology of the gastrointestinal tract, six key markers of damage were assessed in adult zebrafish: disruption of brush border and surface enterocytes, infiltration of polymorphonuclear cells and lymphocytes, dilation of lymphatics and capillaries, edema, villus fusion and villus atrophy. Both lines of adult zebrafish (Tg(*cyp2k18:egfp*) and wildtype AB) ( $n = 6/\text{group}$ ) treated with afinatib did not display histopathological damage to the intestines ( $P > 0.05$ ) (Figure 3(a)). Both lines of adult zebrafish (Tg(*cyp2k18:egfp*) ( $P = 0.0076$ ) and wildtype AB ( $P = 0.0407$ )) treated with SN38 had significantly increased histopathological scores (Figure 3(b) and (c)) compared to controls (Figure 3(d)). The adult Tg(*cyp2k18:egfp*) zebrafish were not different from the wild type (AB) with DMSO control or SN38 or afinatib treatment ( $P > 0.05$ ). To assess the effect of cancer

drugs on goblet cells in the gastrointestinal tract, AB-PAS staining was analyzed. There was no significant difference between either the transgenic ( $5.736 \pm 1.49$  cells per villus in DMSO IP;  $7.446 \pm 1.092$  cell per villus in DMSO gavage) or AB controls ( $5.923 \pm 2.06$  cells per villus in DMSO IP;  $7.625 \pm 1.205$  cells per villus DMSO gavage). There was no significant difference in fish treated with either SN38 ( $8.454 \pm 1.229$  per villus in AB fish;  $6.528 \pm 2.135$  per villus in Tg(*cyp2k18:egfp*) fish), or afinatib ( $5.508 \pm 1.482$  cells per villus in AB fish;  $6.392 \pm 1.957$  cells per villus in Tg(*cyp2k18:egfp*) fish), ( $P > 0.05$ ). Caspase 3 staining to identify apoptotic cells in the intestine showed no significant difference between either the transgenic or wildtype line in controls and fish treated with either SN38 or afinatib ( $P > 0.05$ ; data not shown).

### Discussion

Gastrointestinal toxicity is a common side effect of cancer therapies, and can restrict administration dose, and thus treatment efficacy. There is a pressing need for diverse models and assays to better understand the mechanisms and identify toxicity early in drug development. The zebrafish model has been recognized as a powerful tool for human disease modeling, toxicology and drug screening assays, based largely on its ease of handling, fecundity, low cost, rapid external development, amenability to genetic manipulation as well as its genetic similarity to higher vertebrates.<sup>24</sup> There has been minimal use of the zebrafish model to study gastrointestinal toxicity, with one model reporting mucositis findings when developing a hand-foot disease model with PEGylated doxorubicin.<sup>23</sup> Here, we aimed to utilize a newly developed transgenic reporter line as a novel model to screen anti-cancer drugs that induce gastrointestinal toxicity.

The Tg(*cyp2k18:egfp*) reporter line was developed to screen liver toxicity drugs; however, on testing it was noted that eGFP was also induced in the gastrointestinal

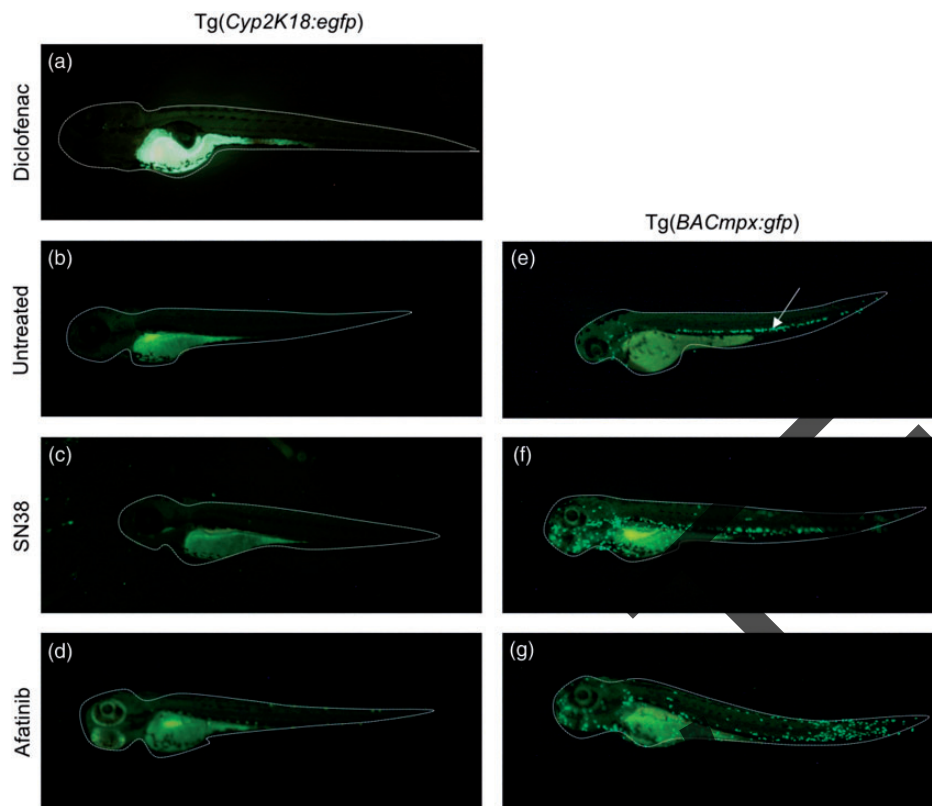


**Figure 2.** Fluorescent microscope still images of Tg(*cyp2k18:egfp*) and Tg(*BACmpx:gfp*) larvae zebrafish at 4 dpf. (a) Diclofenac (positive control) induced eGFP in gastrointestinal tract of Tg(*cyp2k18:egfp*). (b) Untreated larvae did not display eGFP in gastrointestinal tract Tg(*cyp2k18:egfp*). (c) SN38 treatment did not induce eGFP in gastrointestinal tract Tg(*cyp2k18:egfp*). (d) Afatinib treatment did not induce eGFP in gastrointestinal tract Tg(*cyp2k18:egfp*). (e) White arrow: Untreated Tg(*BACmpx:gfp*) displayed neutrophils contained to the vasculature. (f) SN38 treated Tg(*BACmpx:gfp*) displayed some neutrophil translocation from the vasculature. (g) Afatinib treated Tg(*BACmpx:gfp*) displayed neutrophil translocation from the vasculature. (A color version of this figure is available in the online journal.)

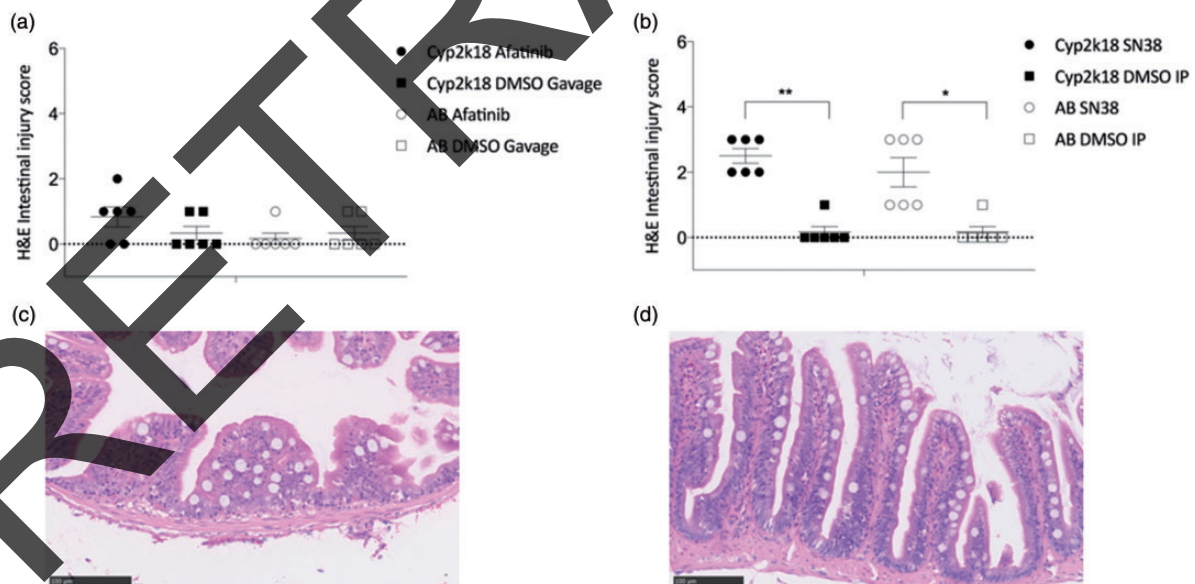


**Figure 3.** Histopathological injury in zebrafish. (a) Adult Tg(*cyp2k18:egfp*) and adult AB zebrafish treated with SN38 had significant histopathological intestinal injury compared to controls (\*\* $P = 0.0076$  and \* $P = 0.0407$ , respectively). (b) Adult zebrafish treated with afatinib did not develop histopathological intestinal injury ( $P > 0.05$ ). (c) Representative image of adult Tg(*cyp2k18:egfp*) zebrafish treated with DMSO control. (d) Representative image of adult Tg(*cyp2k18:egfp*) zebrafish treated with SN38. (A color version of this figure is available in the online journal.)

tract if toxicity was induced.<sup>5</sup> Non-steroidal anti-inflammatory agents such as diclofenac have long been reported to induce gastrointestinal injury.<sup>25</sup> It was therefore logical to

test the ability of this line as a reporter line for cancer treatments that induce both hepatotoxicity and gastrointestinal toxicity. In this model, two agents known to induce severe

gastrointestinal-toxicity were used to assess the viability of the Tg(*cyp2k18:egfp*) line as a high throughput, low-cost screening tool. However, upon testing, it was noted that following treatment with both chosen drugs, SN38 and afatinib, no induction of eGFP was seen in larvae. It is now becoming appreciated that each toxicant is likely to induce a unique set of transcriptional responses and that a global toxic reporter is unlikely to exist. It was noted previously that diverse toxicity reporter lines each responded differently to hepatotoxicants.<sup>5</sup> Ideally any toxicity assay would involve a number of independent reporter lines. Unbiased transcriptional profiling of the toxic response to afatinib and SN38 in the zebrafish might yield novel markers for transgenic reporter development.

A key drawback in using zebrafish for the study of toxicity is that larvae must receive the compound in water. Drug solubility is therefore a major factor to be considered when utilizing this model. While this study overcame this limitation in adult fish by administering drugs via oral gavage or intraperitoneal injection, such approaches are not feasible in larvae nor are adults readily screenable for reporter eGFP induction due to inherent opacity. While it is understood that SN38 and afatinib engage a different pathway for metabolism than Cyp2K18, these agents have been shown to induce hepatotoxicity in other models, the precise mechanisms of which are unknown.<sup>26,27</sup> Therefore, the potential confounding issue in this model may be that sufficient concentrations were not achieved to induce liver or gastrointestinal toxicity due to the low solubility, and thus lack of absorption. The solubility of SN38 has previously been identified as problematic, and hence development of soluble SN38 is now being investigated, and may be useful in this model in the future.<sup>28</sup> Nevertheless, afatinib was soluble, and indeed, caused some lethality at doses above 200  $\mu\text{M}$ ; however, it is unclear if the lethality was of gastrointestinal origin.

Adult zebrafish treated with afatinib did not show histopathological damage. There are a number of reasons to potentially explain this: (1) histopathological damage is only occasionally reported as a feature of targeted-therapy-induced gastrointestinal toxicity; (2) when histopathology is reported, it is most commonly only in the ileum, and it is possible that given the differences in zebrafish gastrointestinal anatomy this was not seen. The zebrafish lacks a stomach, with the regionalization of the adult zebrafish being more gradual. The morphology of the zebrafish intestine is analogous to the villus structure of mammalian intestines, with capacious folds of the epithelium that protrude into the lumen, increasing the surface area with the finger-like projections, however do not contain crypts<sup>8</sup>; (3) afatinib is typically administered daily over many weeks, and so a single dose may not cause gastrointestinal toxicity. Further, studies are therefore needed to further investigate this model with a time-course; however, the tolerance of daily gavage to zebrafish is unclear. Adult zebrafish treated with SN38 showed histopathological damage that is consistent with that seen in mammalian models. The well-characterized features of cancer treatment-induced gastrointestinal histopathological include villous fusion, villous atrophy, disruption of brush border and

surface enterocytes, crypt loss/architectural disruption, disruption of crypt cell, infiltration of polymorphonuclear cells and lymphocytes, dilation of lymphatics and capillaries and edema.<sup>29</sup>

While a robust and tractable genetic model of gastrointestinal toxicity is not available yet, the identification of genes required for the rapid proliferation of zebrafish intestinal epithelial cells during development has highlighted a number of essential genes that could be targeted to disable gastrointestinal toxicity.<sup>30</sup> Moreover, appreciation of the utility of zebrafish to study intestinal inflammation is gaining momentum. In particular, zebrafish provide opportunities to investigate the integrity of intestinal epithelial barrier function, a key emerging marker of gastrointestinal toxicity secondary to cancer treatment, with FITC-dextran gavage. With currently available tools, the interplay between epigenetic regulators, intestinal injury, microbiota composition, and innate immune cell mobilization can be analyzed in exquisite detail.<sup>30</sup> This provides excellent opportunities to define critical events that could be targeted therapeutically. Furthermore, the use of zebrafish larvae as hosts for xenografts of human tissue, while still in its infancy, holds great promise that zebrafish could provide a practical, preclinical personalized medicine platform for the rapid assessment of the drug sensitivity of the patient. Furthermore, there are nascent, yet encouraging, efforts to generate humanized transgenic zebrafish lines for more accurate reconstitution of human drug metabolism.<sup>31</sup>

## Conclusion

Zebrafish are providing several productive avenues for toxicology research; however, a timely screening model for gastrointestinal toxicity second to cancer treatment is yet to be developed. Here, we aimed to utilize a newly developed transgenic reporter line to address this need; however, the transgenic line did not report gastrointestinal toxicity using the compounds tested. This may be explained due to poor solubility, providing an unclear picture of whether these larvae were induced for any type of injury. We therefore had to concentrate our attention on the adult fish in the direct delivery of the compounds. Chemotherapy agents with high solubility and permeability would be more amenable to these models. In addition, different drugs may invoke highly unique genomic responses, and hence we did not see induction of eGFP in larvae in response to these compounds. Further progress in this area would be greatly facilitated by the generation of robust and reproducible genetic models of zebrafish intestinal toxicity that mimic the known pathobiological pathways in rodents and humans, and can be readily induced in a short time-frame. This would include identification of more gastrointestinal toxicity reporter genes in zebrafish from these and other drugs. Suitably apt models will have the potential to enhance the development of novel cancer drugs by providing a platform for high-throughput chemical screens.

**Authors' contributions:** This research was first published in abstract format "Harnessing transgenic zebrafish as a novel platform for the study of chemotherapy- and targeted

therapy-induced gastrointestinal toxicity" in *Abstracts of the MASCC/ISOO Annual Meeting 2018* in the *Supportive Care in Cancer Journal*.<sup>32</sup> All authors participated in the design, interpretation of the studies and analysis of the data and review of the manuscript; YZAVS wrote and received the grants for this study, developed the concept, conducted the experiments and wrote the manuscript, RJG and HRW reviewed manuscript drafts, TJC developed the transgenic reporter line and supplied critical reagents and reviewed manuscript drafts, JMB was involved in developing the concept, and reviewing manuscript drafts.

#### DECLARATION OF CONFLICTING INTERESTS

The author(s) declared the following potential conflicts of interest with respect to the research, authorship, and/or publication of this article: Ysabella Van Sebille declares that she has no conflict of interest. Rachel Gibson declares that she has no conflict of interest. Hannah Wardill declares that she has no conflict of interest. Thomas Carney declares that he has no conflict of interest. Joanne Bowen declares that she has no conflict of interest.

#### FUNDING

The author(s) disclosed receipt of the following financial support for the research, authorship, and/or publication of this article: This study was funded by the Florey Medical Research Foundation Project Grant in Cancer Research. Dr Ysabella Van Sebille was supported by The Australian Postgraduate Award, The Global Learning Travel Grant, The Research Abroad Scholarship, and The Walter and Dorothy Duncan Trust Travel Grant.

#### ORCID iD

Ysabella ZA Van Sebille  <https://orcid.org/0000-0002-5803-3230>

Joanne M Bowen  <https://orcid.org/0000-0003-0876-0031>

#### REFERENCES

- Van Sebille YZ, Gibson RJ, Wardill HR, Bowen JM. Gastrointestinal toxicities of first and second-generation small molecule human epidermal growth factor receptor tyrosine kinase inhibitors in advanced non-small cell lung cancer. *Curr Opin Support Palliat Care* 2016;**10**:152–6
- Lalla RV, Bowen J, Barasch A, Elting L, Epstein J, Keefe DM, McGuire DB, Miglioni C, Nicolatou-Galitis O, Peterson DE, Raber-Durlacher JE, Sonis ST, Elad S. MASCC/ISOO clinical practice guidelines for the management of mucositis secondary to cancer therapy. *Cancer* 2014;**120**:1453–61
- Al-Dasooqi N, Sonis ST, Bowen JM, Bateman E, Blijlevens N, Gibson RJ, Logan RM, Nair RG, Stringer AM, Yazbec R, Elad S, Lalla RV. Emerging evidence on the pathobiology of mucositis. *Support Care Cancer* 2013;**21**:2075–83
- Wardill HR, Gibson RJ, Van Sebille YZ, Secombe KR, Logan RM, Bowen JM. A novel in vitro platform for the study of SN38-induced mucosal damage and the development of Toll-like receptor 4-targeted therapeutic options. *Exp Biol Med* 2016;**241**:1386–94
- Poon KL, Wang X, Lee SG, Ng AS, Goh WH, Zhao Z, Al-Haddawi M, Wang H, Mathavan S, Ingham PW, McGinnis C, Carney TJ. Editor's highlight: transgenic zebrafish reporter lines as alternative in vivo organ toxicity models. *Toxicol Sci* 2017;**156**:133–48
- Wallace KN, Akhter S, Smith EM, Lorent K, Pack M. Intestinal growth and differentiation in zebrafish. *Mech Dev* 2005;**122**:157–73
- Noaillac-Depeyre J, Gas N. Electron microscopic study on gut epithelium of the tench (*Tinca tinca* L.) with respect to its absorptive functions. *Tissue Cell* 1976;**8**:511–30
- Wang Z, Du J, Lam SH, Mathavan S, Matsudaira P, Gong Z. Morphological and molecular evidence for functional organization along the rostrocaudal axis of the adult zebrafish intestine. *BMC Genom* 2010;**11**:392
- Umezawa T, Kiba T, Numata K, Saito T, Nakaoka M, Shintani S, Sekihara H. Comparisons of the pharmacokinetics and the leukopenia and thrombocytopenia grade after administration of irinotecan and 5-fluorouracil in combination to rats. *Anticancer Res* 2000;**20**:4235–42
- Gibson RJ, Bowen JM, Alvarez E, Finnie J, Keefe DM. Establishment of a single-dose irinotecan model of gastrointestinal mucositis. *Chemotherapy* 2007;**53**:360–9
- Araki E, Ishikawa M, Iigo M, Koide T, Itabashi M, Hoshi A. Relationship between development of diarrhea and the concentration of SN-38, an active metabolite of CPT-11, in the intestine and the blood plasma of athymic mice following intraperitoneal administration of CPT-11. *Jpn J Cancer Res* 1993;**84**:697–702
- Pedroso SH, Vieira AT, Bastos RW, Oliveira JS, Cartelle CT, Arantes RM, Soares PM, Generoso SV, Cardoso VN, Teixeira MM, Nicoli JR, Martins FS. Evaluation of mucositis induced by irinotecan after microbial colonization in germ-free mice. *Microbiology*. 2015;**161**:1950–60
- Wind S, Schnell D, Ebner T, Freiwald M, Stopfer P. Clinical pharmacokinetics and pharmacodynamics of afatinib. *Clin Pharmacokinet* 2017;**56**:235–50
- Kimmel CB, Ballard WW, Kimmel SR, Ullmann B, Schilling TF. Stages of embryonic development of the zebrafish. *Dev Dyn* 1995;**203**:253–310
- Renshaw SA, Loynes CA, Trushell DM, Elworthy S, Ingham PW, Whyte MK. A transgenic zebrafish model of neutrophilic inflammation. *Blood* 2006;**108**:3976–8
- Collymore C, Rasmussen S, Tolwani RJ. Gavaging adult zebrafish. *J Vis Exp* 2013;78
- White RM, Sessa A, Burke C, Bowman T, LeBlanc J, Ceol C, Bourque C, Dovey M, Goessling W, Burns CE, Zon LI. Transparent adult zebrafish as a tool for in vivo transplantation analysis. *Cell Stem Cell* 2008;**2**:183–9
- Wardill HR, Bowen JM, Van Sebille YZ, Secombe KR, Coller JK, Ball IA, Logan RM, Gibson RJ. TLR4-dependent claudin-1 internalization and secretagogue-mediated chloride secretion regulate irinotecan-induced diarrhea. *Mol Cancer Ther* 2016;**15**:2767–79
- Gibson RJ, Bowen JM, Inglis MR, Cummins AG, Keefe DM. Irinotecan causes severe small intestinal damage, as well as colonic damage, in the rat with implanted breast cancer. *J Gastroenterol Hepatol* 2003;**18**:1095–100
- Keefe DM, Brealey J, Goland GJ, Cummins AG. Chemotherapy for cancer causes apoptosis that precedes hypoplasia in crypts of the small intestine in humans. *Gut* 2000;**47**:632–7
- Logan RM, Gibson RJ, Bowen JM, Stringer AM, Sonis ST, Keefe DM. Characterisation of mucosal changes in the alimentary tract following administration of irinotecan: implications for the pathobiology of mucositis. *Cancer Chemother Pharmacol* 2008;**62**:33–41
- Bowen JM, Mayo BJ, Plews E, Bateman E, Wignall A, Stringer AM, Boyle FM, Keefe DM. Determining the mechanisms of lapatinib-induced diarrhoea using a rat model. *Cancer Chemother Pharmacol* 2014;**74**:617–27
- Chen YH, Lee YT, Wen CC, Chen YC, Chen YJ. Modeling pegylated liposomal doxorubicin-induced hand-foot syndrome and intestinal mucositis in zebrafish. *Oncotargets Ther* 2014;**7**:1169–75
- Santoriello C, Zon LI. Hooked! Modeling human disease in zebrafish. *J Clin Invest* 2012;**122**:2337–43
- Matsui H, Shimokawa O, Kaneko T, Nagano Y, Rai K, Hyodo I. The pathophysiology of non-steroidal anti-inflammatory drug (NSAID)-induced mucosal injuries in stomach and small intestine. *J Clin Biochem Nutr* 2011;**48**:107–11
- Takeda M, Nakagawa K. Toxicity profile of epidermal growth factor receptor tyrosine kinase inhibitors in patients with epidermal growth factor receptor gene mutation-positive lung cancer. *Mol Clin Oncol* 2017;**6**:3–6



27. Cai Z, Yang J, Shu X, Xiong X. Chemotherapy-associated hepatotoxicity in colorectal cancer. *J Buon* 2014;**19**:350-6
28. Bala V, Rao S, Prestidge CA. Facilitating gastrointestinal solubilisation and enhanced oral absorption of SN38 using a molecularly complexed silica-lipid hybrid delivery system. *Eur J Pharm Biopharm* 2016;**105**:32-9
29. Van Sebille YZA, Gibson RJ, Wardill HR, Secombe KR, Ball IA, Keefe DM, Finnie JW, Bowen JM. Dacomitinib-induced diarrhoea is associated with altered gastrointestinal permeability and disruption in ileal histology in rats. *Int J Cancer* 2017;**140**:2820-9
30. Lobert VH, Mouradov D, Heath JK. Focusing the spotlight on the zebrafish intestine to illuminate mechanisms of colorectal cancer. *Adv Exp Med Biol* 2016;**916**:411-37
31. Poon KL, Wang X, Ng AS, Goh WH, McGinnis C, Fowler S, Carney TJ, Wang H, Ingham PW. Humanizing the zebrafish liver shifts drug metabolic profiles and improves pharmacokinetics of CYP3A4 substrates. *Arch Toxicol* 2017;**91**:1187-97
32. Van Sebille YZA, Bowen JM, Gibson RJ, Wardill HR, Carney TJ. Harnessing transgenic zebrafish as a novel platform for the study of chemotherapy- and targeted therapy- induced gastrointestinal toxicity. *Support Care Cancer* 2018;**26**:S39-S364

(Received March 21, 2019, Accepted May 15, 2019)

RETRACTED